

## Localized Region Based Active Contour Algorithm for Segmentation of Abdominal Organs and Tumors in Computer Tomography Images

<sup>1</sup>S.N. Kumar, <sup>2</sup>A. Lenin Fred, <sup>1</sup>S. Lalitha Kumari, <sup>3</sup>P. Sebastian Varghese

<sup>1</sup>Department of ECE, Sathyabama University, Chennai, Tamil Nadu, India

<sup>2</sup>Department of CSE, Mar Ephraem College of Engineering and Technology, Marthandam, Tamil Nadu, India

<sup>3</sup>Consultant Radiologist Metro Scans and Laboratory, Thiruvananthapuram, Kerala, India

---

**Abstract:** This study presents a localized region based lankton algorithm with decision median filter for the segmentation of abdominal organs and tumors in CT images. Active contour algorithms based on discrete representation of implicit functions are widely used in medical image segmentation. The decision median filter can filter the gaussian noise and impulse noise efficiently than conventional spatial domain filters with better edge preservation. A comparative analysis of various active contour models is done and the decision median filter based lankton segmentation algorithm gives best result. The performance of the proposed segmentation algorithm was evaluated in terms of metrics like dice coefficient and hausdorff distance. The proposed algorithm effectively segments the abdominal organs and tumors in computer tomography images with well-defined boundaries.

**Key words:** Image segmentation, curve evolution, filtering, level set methods, region

---

### INTRODUCTION

Image segmentation is the process of grouping the pixels in an image into a set of disjoint regions with uniform and homogeneous attributes such as intensity, color, tone or texture etc. The medical image segmentation algorithms plays a vital role in diagnosis and radiation therapy since they are used to localize the tumor region and other anomalies; measure tissue volumes and analysis of anatomical structures. In many cases the segmentation algorithms result are prone to error because of noisy images. The noise in CT images are generally modelled as gaussian noise, however in many cases the noise deviates from gaussian distribution and it can be defined as graininess, speckle or impulse noise (Shinde *et al.*, 2012; Prasad and Ganesan, 2013) Median filter and Gaussian filter are widely used spatial domain filter in the noise removal of CT images (Kalra *et al.*, 2003; Denis *et al.*, 2012; Lin *et al.*, 2006; Wang and Zhang, 1999). The Active contour models are broadly classified in to two types: Parametric models and geometric models (Shih and Zhang, 2004, 2007). The snake is a parametric active contour model in which the initial contour points should be placed closer to the true boundary (Shih and Zhang, 2004, 2007). The curve evolution in parametric active contour has discrepancies when it encounters in to

boundary concavities and complex topological structures (Shih and Zhang, 2004, 2007). Many research works had undergone to overcome the issues in traditional snake parametric models. Level set is a geometric active contour technique in which a discrete set of control points are used to initialize a curve which will evolve to enclose the desired region of interest (Tsai and Osher, 2003). The region based active contour model is insensitive to noise and independent of initial contour position (Chan and Vese, 2001; Lankton and Tannenbaum, 2008). The issues in global region based models like failing to detect the objects of low contrast and non-uniform illumination are overcome by local region based active contour models (Chan and Vese, 2001; Lankton and Tannenbaum, 2008). The modification of energy function in level set algorithms were made for the segmentation and bias field estimation in MR images with intensity in homogeneity (Li *et al.*, 2011; Cui *et al.*, 2013; Qian *et al.*, 2013). The region based level set algorithm based on global and local information was developed for the segmentation of images with low contrast and intensity inhomogeneity (Zhao *et al.*, 2012; Liu *et al.*, 2014; Barman *et al.*, 2011; Tamimi and Sulong, 2014).

A comparative analysis of various level set methods was done to detect the boundary of cell in medical images

(Gurari *et al.*, 2015). The caselles active contour model uses gradient of the image to determine the energy function and the curve is evolved into the regions of high gradient (Caselles *et al.*, 1997). The Chan and Vese model is a region based model in which the image is subdivided into two homogeneous regions based on the energy constraints and the curve evolution is based on the narrow band of level set (Chan and Vese, 2001). The Shi algorithm is very fast method and the curve evolution takes place in narrow band (Shi and Karl, 2008). In Bernard algorithm the energy function minimization is done with respect to B-spline coefficients (Bernard *et al.*, 2008). The Lankton and li algorithm evolve the initial contour based on the local neighbourhood statistics and can segment the image in to two homogeneous regions (Lankton *et al.*, 2008; Li *et al.*, 2008).

**MATERIALS AND METHODS**

**Acquisition protocol:** The CT images have been acquired on optima CT machine. Both plain and contrast enhanced CT images are taken with 0.6 mm slice thickness. The patient consent was obtained for publishing the images. The abdominal CT images of 5 data sets were used which comprises of three data sets of malignant renal cell tumour (Renal cell carcinoma) and two data sets of malignant liver tumour (Hepatic cellular carcinoma). The pre-processing along with segmentation algorithm was applied on all the 5 data set and the result of typical slices are depicted in the results and discussion. The ethics committee for biomedical activities of mar ephraem international center for medical image processing and metro scans and laboratory, Thiruvananthapuram approved the study of CT images of human subjects for research work.

**Preprocessing:** The median filter is a conventional spatial domain nonlinear filter that replaces each pixel by the median of the gray levels in the neighbourhood of that pixel and it is independent of the characteristics of the image and it is efficient for low noise intensity. The median filter alters the non-noisy pixel gray level values unnecessarily and in the case of gaussian filter, the edge preservation is poor (Kalra *et al.*, 2003). The adaptive median filter outperforms the median filter by taking into account of the statistical characteristics of the image (Lin *et al.*, 2006; Wang and Zhang, 1999). The size of the kernel in adaptive median filter changes with respect to the noisy pixels and non-noisy pixels, however the adaptive median filter produces blurring effect in the case of images with high noise intensity (Lin *et al.*, 2006; Wang and Zhang, 1999). The choice of filter depends upon the medical image modality and the nature of noise

(Lin *et al.*, 2006; Wang and Zhang, 1999). The Progressive Switching Median Filter (PSMF) does not alter the non-noisy pixels unless like conventional median filter (Wang and Zhang, 1999). The decision median filter operation comprises of two stages Noise detection, Noise filtering and it is free from the crucial parameter selection unlike PSMF (Wang and Zhang, 1999). The steps in decision based median filter can be summarized as follows:

- Step 1:** Choose a 2D window of size 3×3 and  $P_{ij}$  be the processing pixel
- Step 2:** Determine the minimum ( $P_{min}$ ) and maximum ( $P_{max}$ ) gray value of pixels in the processing window
  - If  $P_{min} < P_{ij} < P_{max}$  the pixel gray value ( $P_{ij}$ ) is left unchanged, else move to the next step
- Step 3:** If  $P_{ij} = P_{min}$  or  $P_{ij} = P_{max}$  or, then the following condition is evaluated
  - When the neighbourhood pixel gray values in the mask are same as  $P_{ij}$  then it is a non-noisy pixel and is left unchanged, otherwise move to the next step
- Step 4:** When  $P_{ij}$  is a corrupted pixel, there are two possible cases
  - Case i: Replace  $P_{ij}$  with the mean of the elements in the window, if the neighbourhood Pixels gray value are  $P_{min}$  and  $P_{max}$ .
  - Case ii: Replace  $P_{ij}$  with the median value, when all the neighbourhood pixels gray value are not  $P_{min}$  and  $P_{max}$ . The median is determined from the elements in the window while discarding the pixels with gray value  $P_{min}$  and  $P_{max}$ .
- Step 5:** Repeat steps 1-4 until all the pixels in the image are processed.

**Localized region active contour model:** Shawn Lankton et al developed an active contour model taking into account of the local statistics for the segmentation of neural fibre bundles in Diffusion Weighted Magnetic Resonance Images (DW-MRI) (Lankton *et al.*, (2008). Lankton active contour algorithm is a region based technique in which the contour evolution is determined by neighbourhood pixel statistical features Lankton *et al.* (2008). The lankton algorithm is based on the assumption that pixel features inside the initially drawn contour will have homogeneous characteristics when compared to the pixels outside the contour. When the pixel characteristics are heterogeneous inside the contour, region based active contour algorithms will not be able to efficiently segment the desired object. The ball function in terms of the global radius  $\rho$  is used to model the local statistics features:

$$\beta\left(\frac{x}{y}\right) = \begin{cases} 1; & x - y < \rho \\ 0; & \text{otherwise} \end{cases} \quad (1)$$

The radius ‘ $\rho$ ’ is set to small while comparing to the structure to be segmented and  $\beta(x, y)$  is used to mask local regions. The ball function value is ‘1’ when the point  $y$  is within a ball of radius ‘ $\rho$ ’ centered at  $x$  and ‘0’ otherwise. The ball function is used in conjunction with the heavy side smoothing function  $\psi_H(x)$  to select interior and exterior region:

$$\psi_H(x) = \begin{cases} 1 & 1; \psi(x) < -\epsilon \\ 0 & 0; \psi(x) < \epsilon \\ \frac{1}{2} \left[ 1 + \frac{\psi}{\epsilon} + \frac{1}{\psi} \sin\left(\frac{\pi \psi(x)}{\epsilon}\right) \right] & \text{otherwise} \end{cases} \quad (2)$$

Let  $\psi_H(y)$  denotes the interior region of the evolving contour and  $\psi_H'(y)$  corresponds to the exterior region of the evolving contour:

$$\psi_H'(y) = 1 - \psi_H(y) \quad (3)$$

The local interior and local exterior at point  $x$  can be expressed in terms of  $\beta(x, y)$  and  $\psi_H(y)$ :

$$l(i) = \beta(x, y) \times \psi_H(y) \quad (4)$$

$$l(e) = \beta(x, y) \times (1 - \psi_H(y)) \quad (5)$$

Where:

$l(i)$  = Local interior at point  $x$  and

$l(e)$  = The local exterior at point  $x$

The energy criterion in terms of the signed distance function  $\phi$  is as follows:

$$E(\phi) = \int_{O_x} d\psi(x) \times \int_{O_y} \beta(x, y) F[f(y), \psi(y)] dy dx + \lambda \int_{O_x} d\psi(x) \nabla \psi(x) dx \quad (6)$$

where, first term is data attached term and  $\delta$  is the dirac function, second term is the usual regularise term that smooth the contour. Chan and features yezzi features:

$$F[f(y), \psi(y)] = \begin{cases} \psi_H(y)(f(y) - v(x))^2 + (1 - \psi_H(y)) \\ (f(y) - u(x))^2; (v(x) - u(x))^2 \end{cases} \quad (7)$$

Where:

$H$  = The heavy side function

$u(x)$  and  $v(x)$  = Anterior and exterior mean updated at each iterations as follow

$$u(x) = \frac{\int \beta(x, y) \psi_H(y) f(y) dy}{\int \beta(x, y) \psi_H(y) dy} \quad (8)$$

$$v(x) = \frac{\int \beta(x, y) (1 - \psi_H(y)) f(y) dy}{\int \beta(x, y) (1 - \psi_H(y)) dy} \quad (9)$$

The energy function minimization is done by calculus of variation and it is governed by gradient descent curvature flow computation.

The curve evolution is as follows:

$$\frac{d\psi(x)}{dt} = d(\psi(x)) \int \beta(x, y) \nabla \psi F(f(y), \psi(y)) dy + \lambda \delta(\psi(x)) \quad (10)$$

Where:

$$\nabla \psi F(f(y), \psi(y)) = \begin{pmatrix} d(\psi(y))(f(y) - v(x))^2 - (f(y) - u(x))^2 \\ d(\psi(y)) \frac{(f(y) - v(x))^2}{S_v} \\ - \frac{(f(y) - u(x))^2}{S_u} \end{pmatrix} \quad (11)$$

The local interior and local exterior area is modelled by  $A_v$  and  $A_u$ :

$$S_v = \int \beta(x, y) (1 - \psi_H(y)) dy \quad (12)$$

$$S_u = \int \beta(x, y) \psi_H(y) dy \quad (13)$$

where, the  $\lambda$  is the curvature term and it influence the regularization term of evolving contour. The size of the neighbourhood is fixed by the radius term  $\rho$ . The lanktoncurve evolution algorithm is able to segment the abdominal organs and anomalies with good edge preservation.

## RESULTS AND DISCUSSION

The segmentation was done by various active contour approaches and comparative study of performance of active contour algorithms was also done (Barman *et al.*, 2011). Prior to segmentation, the pre-processing was done by decision median filter for filtering the noise. A comparative analysis of six active contour models was done by creaseg software to evaluate the segmentation result (Dietenbeck *et al.*, 2010). The level set algorithms are classified based on the data attachment type and the curve evolution nature. The data attachment type determines the curve evolution phenomena and it may be contour information (based on gradient function) or region information (based on statistical features). Chan and Vese, Bernard and Shi algorithm are region based active contour model and Caselles is a contour based active contour model. Lankton and Li algorithm are localized region based active contour

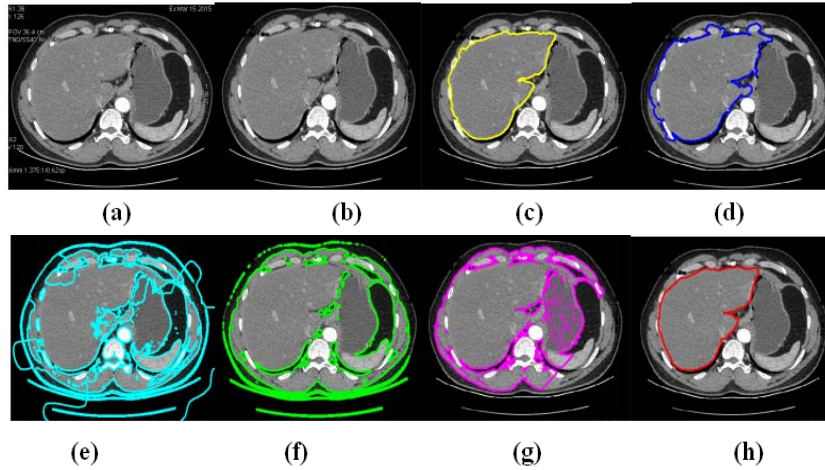


Fig. 1: a) Input slice (case 1(s1)); b) preprocessed image; c) Caselles output; d) Chan and vese output; e) Chimming Li output; f) Bernard output; g) Shi output; f) Lanktonoutput

model. The curve evolution in bernard and li algorithm takes place in whole domain while in the case of remaining active contour models the curve evolution takes place in narrow band.

The Dice Coefficient (DC) is a measure to indicate the percentage of spatial overlap between the segmented image and ground truth image. The dice coefficient is given by Eq. 14:

$$D = \frac{2(S \cap G)}{(S \cap G + S \cup G)} \quad (14)$$

where, S and G is the segmented image and ground truth image. Hausdorff distance is a good measure to analyse the performance of segmentation algorithm. The symmetric hausdorff distance is given by Eq. 15:

$$d_s = \max(d(S,G), d(G,S)) \quad (15)$$

where,  $d(S, G) = \max_{s \in S} \min_{g \in G} \|s-g\|$  and  $d(G, S) = \max_{g \in G} \min_{s \in S} \|s-g\|$ . The function  $d(S, G)$  is the directed hausdorff distance from S to G. The hausdorff distance  $d_s(S, G)$  is the maximum of  $d(S, G)$  and  $d(G, S)$ . The ground truth image is obtained by manual delineation by the radiologist who carefully trace the boundaries of abdominal organs and abnormalities. The input slices of data set 1 with different cross section of liver are taken in to account for the analysis of active contour segmentation algorithms.

The input image is pre-processed by decision based median filter. Figure 1 depicts the liver segmentation result of various active contour approaches of dataset1

corresponding to a typical input slice depicting the liver at the level of fissure for ligamentum venosum. For the curve evolution in lankton algorithm was used with and equal to 9. The qualitative inspection by expert radiologist shows that the lankton algorithm gives best result and it is validated by performance metrics.

The dice coefficient value is 1 for perfect segmentation and the segmentation algorithm result is acceptable if  $DC \geq 0.9$ . The hausdorff distance should be minimum and for perfect segmentation, the value is zero. The active contour model result is acceptable if  $HD \geq 15$  as per the Creaseg software. The active contour algorithms are also analyzed on various input slices of dataset 1 and the lankton liver segmentation output of typical input slices are shown in Fig. 2a-d. The dice coefficient and hausdorff distance of various active contour approaches are shown in Table 1. The terms S1-S5 represents the typical slices of data set 1. The Caselles and lankton algorithm produces better results since  $DC > 0.9$  and  $HD < 15$ , however lankton algorithm outperforms the remaining active contour approaches.

The liver tumor segmentation of selective input slices corresponding to dataset 2 (S6) and data set 3(S7) for lankton algorithm are depicted below in Fig 3e, f. The terms S6 and 7 represents the typical slice of data set 2 and 3 and similarly S8 and S9 represents the typical slice of data set 4 and 5.

The lankton segmentation algorithm is analysed on different slices of malignant renal tumor dataset 4(S8) and dataset 5 (S9) and the result of typical slices are depicted in Fig. 3g, h. The dice coefficient and hausdorff distance of active contour approaches of slices corresponding to malignant liver tumor (S6 and 7) and malignant renal tumor

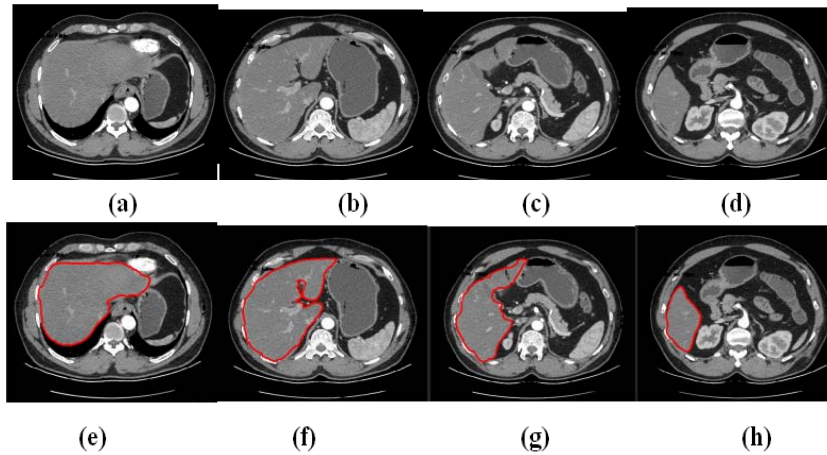


Fig. 2: a) Liver near the level of diaphragm (S2) ;b) liver at the level of fissure for ligamentum trees (S3); c) Liver at the level of gall bladder fossa (S4); d) Inferior pole of liver (S5); e-h) Lankton algorithm result of (a-d)

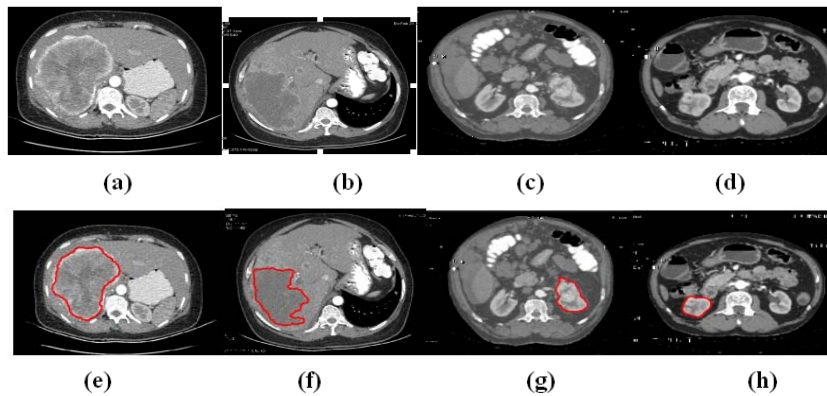


Fig. 3: a-d) Pre-processed input images; e-h) Lankton algorithm results of (a-d)

Table 1: Technical and pathological information of different data sets

ID	x/y/z (mm)	(w/h)×slices	Pathological information
1	0.6	512×128	Renal cell carcinoma , exophytic isodense soft tissue density lesion in the lower pole of right kidney
2	0.6	512×128	Metastasis ,large hypo dense mass lesion in right lobe and caudate lobe
3	0.6	512×128	Metastasis, large hypo dense mass lesion in right lobe and small hypo dense lesions in left lobe
4	0.6	512×128	Renal cell carcinoma, isodense mass lesion with lobulated margins in the lower interpolar region of right kidney
5	0.6	512×128	Renal cell carcinoma, isodense mass lesion with lobulated margins noted in the lower interpolar region of left kidney

Table 2: Dice coefficient and hausdorff distance of active contour approaches for liver segmentation

Active contour algorithms	Dice Coefficient (DC)					Hausdorff distance (HD)				
	S1	S2	S3	S4	S5	S1	S2	S3	S4	S5
Caselles	0.95	0.95	0.96	0.96	0.93	11.24	10.05	9.220	10.08	10.02
Chan and vese	0.88	0.87	0.91	0.88	0.81	16.46	17.32	16.14	18.14	16.14
Chimming Li	0.46	0.31	0.29	0.26	0.24	28.56	30.46	31.24	34.65	33.62
Bernard	0.53	0.52	0.48	0.40	0.50	22.56	24.68	25.43	28.76	26.72
Shi	0.60	0.70	0.63	0.57	0.53	18.23	19.46	18.68	21.45	22.32
Lankton	0.97	0.96	0.97	0.97	0.94	8.240	7.030	7.810	8.220	7.320

(S8 and 9) are depicted in Table 2. In the case of tumor segmentation also the lankton algorithm outperforms the remaining active contour approaches.

Apart from the quantitative analysis of segmentation results by performance metrics, the qualitative analysis was also done by the radiologist and the confirmation of the results was obtained. The lankton localized region

Table 3: Dice coefficient and hausdorff distance of active contour approaches for liver tumor and kidney tumor segmentation

Active contour algorithms	Dice Coefficient (DC)				Hausdorff Distance (HD)			
	S6	S7	S8	S9	S6	S7	S8	S3
Caselles	0.94	0.93	0.89	0.88	12.08	14.06	5.020	4.120
Chan and Vese	0.74	0.77	0.86	0.86	18.67	20.23	5.100	5.240
Chimming Li	0.20	0.21	0.25	0.24	33.67	50.65	20.26	19.24
Bernard	0.40	0.43	0.41	0.39	26.56	36.45	14.46	16.56
Shi	0.50	0.52	0.39	0.40	24.46	32.45	8.560	10.24
Lankton	0.95	0.95	0.930	0.91	9.490	10.56	4.020	3.610

based active contour model can thus segment accurately the anatomical organs of complex shape with better edge preservation.

### CONCLUSION

In this study decision median filter based lankton segmentation algorithm is proposed for the segmentation of abdominal organs and tumor on abdomen CT images. The performance of the algorithm was quantitatively evaluated by appropriate metrics and qualitative evaluation was also done by the experts. A comparative analysis of various active contour models comprising of contour based, region based and localized region based is done in this study. The lankton algorithm gives best results for the segmentation of abdominal organs and tumor on CT images in terms of the performance metrics. The future work will be to incorporate the fuzzy clustering along with the lankton level set approach for a refined result.

### REFERENCES

Barman, P.C., M.S. Miah, B.C. Singh and T. Khatun, 2011. MRI image segmentation using level set method and implement an medical diagnosis system. *Comput. Sci. Eng. Int. J.*, 1: 1-10.

Bernard, O., D. Friboulet, P. Thevenaz and M. Unser, 2008. Variational B-spline level-set method for fast image segmentation. *Proceedings of the 2008 5th IEEE International Symposium on Biomedical Imaging: From Nano to Macro*, May 14-17, 2008, IEEE, France, ISBN: 978-1-4244-2002-5, pp: 177-180.

Caselles, V., R. Kimmel and G. Sapiro, 1997. Geodesic active contours. *Int. J. Comput. Vision*, 22: 61-79.

Chan, T.F. and L.A. Vese, 2001. Active contours without edges. *IEEE Trans. Image Process.*, 10: 266-277.

Cui, W., Y. Wang, T. Lei, Y. Fan and Y. Feng, 2013. Level set segmentation of medical images based on local region statistics and maximum a posteriori probability. *Comput. Math. Methods Med.*, 2013: 1-12.

Denis, T., M.K. Kalra and P.A. Gevenois, 2012. *Radiation Dose from Multidetector CT*. 2nd Edn., Springer, Berlin, Germany, ISBN: 978-3-642-24534-3, Pages: 647.

Dietenbeck, T., M. Alessandrini, D. Friboulet and O. Bernard, 2010. CREASEG: A free software for the evaluation of image segmentation algorithms based on level-set. *Proceedings of the 2010 IEEE International Conference on Image Processing*, September 26-29, 2010, IEEE, France, ISBN: 978-1-4244-7992-4, pp: 665-668.

Gurari, D., D. Theriault, M. Sameki, B. Isenberg and T.A. Pham *et al.*, 2015. How to collect segmentations for biomedical images? A benchmark evaluating the performance of experts, crowdsourced non-experts and algorithms. *Proceedings of the 2015 IEEE Winter Conference on Applications of Computer Vision*, January 5-9, 2015, IEEE, Boston, Massachusetts, ISBN: 978-1-4799-6683-7, pp: 1169-1176.

Kalra, M.K., M.M. Maher, D.V. Sahani, M.A. Blake and P.F. Hahn *et al.*, 2003. Low-dose CT of the abdomen: Evaluation of image improvement with use of noise reduction filters-pilot study 1. *Radiol.*, 228: 251-256.

Lankton, S. and A. Tannenbaum, 2008. Localizing region-based active contours. *IEEE Trans. Image Process.*, 17: 2029-2039.

Lankton, S., J. Melonakos, J. Malcolm, S. Dambreville and A. Tannenbaum, 2008. Localized statistics for DW-MRI fiber bundle segmentation. *Proceedings of the IEEE Computer Society Conference on Computer Vision and Pattern Recognition Workshops CVPRW'08*, June 23-28, 2008, IEEE, Atlanta, USA., pp: 1-8.

Li, C., C.Y. Kao, J.C. Gore and Z. Ding, 2008. Minimization of region-scalable fitting energy for image segmentation. *IEEE. Trans. Image Process.*, 17: 1940-1949.

Li, C., R. Huang, Z. Ding, J.C. Gatenby, D.N. Metaxas and J.C. Gore, 2011. A level set method for image segmentation in the presence of intensity inhomogeneities with application to MRI. *IEEE Trans. Image Process.*, 20: 2007-2016.

- Lin, D.T., C.C. Lei and S.W. Hung, 2006. Computer-aided kidney segmentation on abdominal CT images. *IEEE. Trans. Inf. Technol. Biomed.*, 10: 59-65.
- Liu, T., H. Xu, W. Jin, Z. Liu and Y. Zhao *et al.*, 2014. Medical image segmentation based on a hybrid region-based active contour model. *Comput. Math. Methods Med.*, 2014: 1-10.
- Prasad, S. and N. Ganesan, 2013. An efficient approach for image filtering by using neighbors pixels. *Editorial Preface*, 4: 133-138.
- Qian, X., J. Wang, S. Guo and Q. Li, 2013. An active contour model for medical image segmentation with application to brain CT image. *Med. Phys.*, 40: 1-10.
- Shi, Y. and W.C. Karl, 2008. A real-time algorithm for the approximation of level-set-based curve evolution. *IEEE. Trans. Image Process.*, 17: 645-656.
- Shih, F.Y. and K. Zhang, 2004. Efficient contour detection based on improved snake model. *Int. J. Pattern Recognit. Artif. Intell.*, 18: 197-209.
- Shih, F.Y. and K. Zhang, 2007. Locating object contours in complex background using improved snakes. *Comput. Vision Image Understanding*, 105: 93-98.
- Shinde, B., D. Mhaske and A.R. Dani, 2012. Study of noise detection and noise removal techniques in medical images. *Int. J. Image Graphics Signal Process.*, 4: 51-60.
- Tamimi, A.M.S.H. and G. Sulong, 2014. A review of snake models in medical MR image segmentation. *J. Technol.*, 69: 101-106.
- Tsai, R. and S. Osher, 2003. Review article: Level set methods and their applications in image science. *Commun. Math. Sci.*, 1: 1-20.
- Wang, Z. and D. Zhang, 1999. Progressive switching median filter for the removal of impulse noise from highly corrupted images. *Circuits Syst. II: Analog Digital Signal Process. IEEE Trans.*, 46: 78-80.
- Zhao, Y.Q., X.F. Wang, F.Y. Shih and G. Yu, 2012. A level-set method based on global and local regions for image segmentation. *Int. J. Pattern Recognit. Artif. Intell.*, 26: 1-16.